APPROACH FOR THE ANALYTICAL DESCRIPTION OF THE POST-DAMAGE BEHAVIOUR OF STEEL AND CARBON FIBRE REINFORCED HYBRID COMPOSITES

B. Hannemann[1*], J. Rehra[1], S. Schmeer[1] and U. P. Breuer[1]

[1]Institut für Verbundwerkstoffe GmbH, Erwin-Schrödinger-Str. 58, 67663 Kaiserslautern, Germany
Email: benedikt.hannemann@ivw.uni-kl.de, Web Page: http://www.ivw.uni-kl.de

Keywords: hybrid composite, steel fibres, post-damage behaviour, constitutive law

Abstract

The integration of continuous steel fibres into thin-walled thermoset carbon fibre reinforced polymer (CFRP) enables significant enhancements of its damage tolerance and crashworthiness. Due to their high strain at failure, the embedded steel fibres provide alternative load paths after failure of the brittle carbon fibres. As shown in previous studies, the resulting post-damage performance of the hybrid composite depends on the proportions of the different types of reinforcing fibres, their individual properties, the laminate architecture and particularly on the steel fibre-resin-adhesion. So far, material models provided by common finite element analysis (FEA) tools cannot account for this complex interrelation in an adequate, efficient manner. For this reason, an analytical method is introduced aiming to describe the failure performance of fibre hybrid composites. In principle, the analytical approach is based on a structural dynamic analysis of the fracture gap formation during failure initiation. The present work briefly covers the derivation of this analytical approach and its exemplary application to a steel and carbon fibre reinforced hybrid composite.

1. Introduction

Thermoset CFRP is distinguished by superior weight specific mechanical properties, such as high stiffness and high tensile strength. Under compression load, various failure mechanisms (e.g. fibre fracture, inter-fibre-failure, inter- and intralaminar friction, laminate fragmentation) additionally enable an excellent energy absorption capacity. By contrast, under tensile load, CFRP fails singularly, causing considerable drawbacks regarding structural integrity (disintegration of structures) and crashworthiness. In case of applications with special requirements e.g. regarding the reliability of operation, this might cause an exclusion of CFRP as construction material.

An approach to face this brittle failure behaviour of thermoset CFRP under tensile load comprises the integration of highly ductile continuous steel fibres. Due to their high strain at failure, the embedded steel fibres provide alternative load paths after failure of the brittle carbon fibres; previous experimental studies have shown significant enhancements of the plain tension behaviour of CFRP regarding its ultimate strain at failure ($\varepsilon_{max} > 11$ %) and, as a consequence, energy absorption capacity (E_{abs}: +557 %). The gradual failure behaviour facilitates an increase in e.g. impact and penetration resistance, notch impact performance and load application (fastener pull through, bearing failure). [1-6]

The post damage performance of the hybrid composite, i.e. the stress-strain relation from the beginning of the carbon fibre failure to the catastrophic failure, depends on various parameters, such as the proportions of carbon and steel fibres, their individual mechanical properties, the laminate architecture and the steel fibre-resin-adhesion. Generally, the greater the addressable energy absorption capacity of the steel fibres and the less elastic energy released by the carbon fibres, the more pronounced is the post-damage performance of the hybrid composite. [1, 6]

Despite the complex failure behaviour, the entire stress-strain relation of the hybrid composite has to be predictable in order to exploit its full (mechanical) potential during component design. In principle, a micromechanical simulation of the fibre hybrid composite can consider the complex interaction of the parameters mentioned before [7-8]. However, such analysis requires a very fine meshing, hence computational effort and is therefore limited to small volumes. The calculation of large structures requires more efficient methods with a lower level of detail, i.e. a macro-mechanical modelling. Material laws (e.g. linear elastic, bilinear elastic plastic) of common FEA tools are sufficient to describe the stress-strain relation of the hybrid composite until failure initiation. However, in order to describe the post-damage behaviour, proper failure models for composites which consider local phenomena of the material degradation and in particular the plastic material behaviour of the metal phase are not available.

Against this background, the present paper briefly introduces the basic idea of an analytical approach to describe the material behaviour, particularly the stage after failure initiation, of a steel and carbon fibre reinforced polymer (SCFRP). An elaborated derivation of this analytical approach is given in [9].

2. Theoretical approach

Understanding the macro-mechanical failure behaviour of a steel-carbon-fibre hybrid composite requires a micro-mechanical consideration of its fracture mechanics. For this purpose, the general force-displacement-curve of the tensile-loaded hybrid composite is subdivided into several states, figure 1 (left) and figure 2. The corresponding stress-strain states of the steel and carbon fibres are illustrated in figure 1 (right). In this context, the following simplifications are made:

(1) The carbon fibres as well as the epoxy resin exhibit a linear-elastic stress-strain relation. Both components are perfectly bonded together and fail simultaneously when exceeding the elongation at break of the carbon fibres ($\varepsilon_{max,R} = \varepsilon_{max,CF}$). For convenience, they are considered as combined phase with homogenised properties denominated as surrounding CFRP.

(2) The steel fibres exhibit a non-linear elastic-plastic stress-strain relation. Failure of all steel filaments occurs uniformly when exceeding their strain at failure.

(3) All three components exhibit the same behaviour under compression as under tensile load.

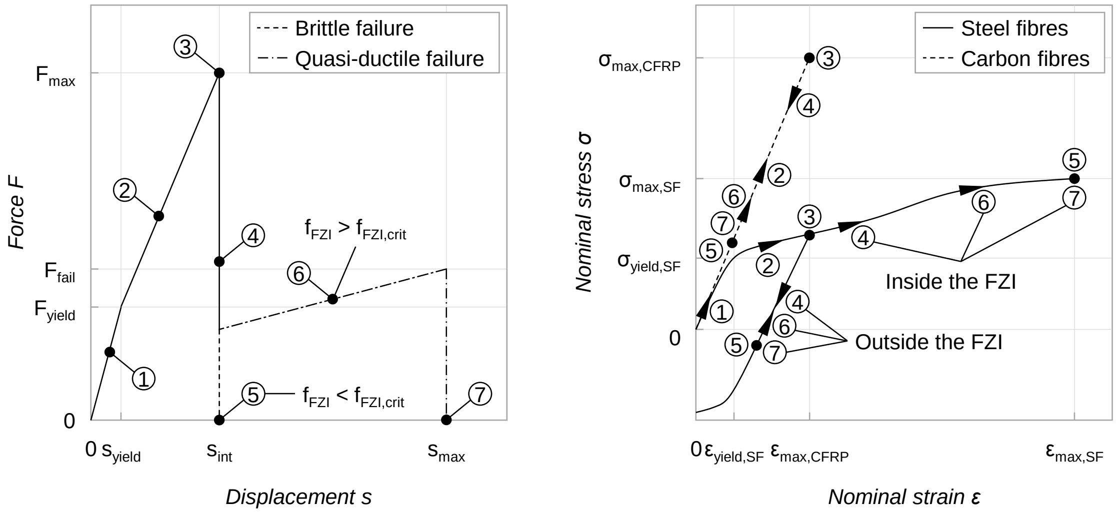

Figure 1. Schematic representation of (left) the force-displacement curve of a UD hybrid composite under tensile load in parallel to the fibre orientation and (right) the corresponding stress-strain states of the embedded steel and carbon fibres [1]

State 1: The global elongation of the composite leads to a homogeneous strain state within the entire hybrid composite; the local elongation of each constituent corresponds to the global deformation of the composite. Initially, both the steel fibres and the surrounding CFRP are elastically elongated. Due to the homogeneous elastic deformation, elastic energy is stored in the entire volume of the material.

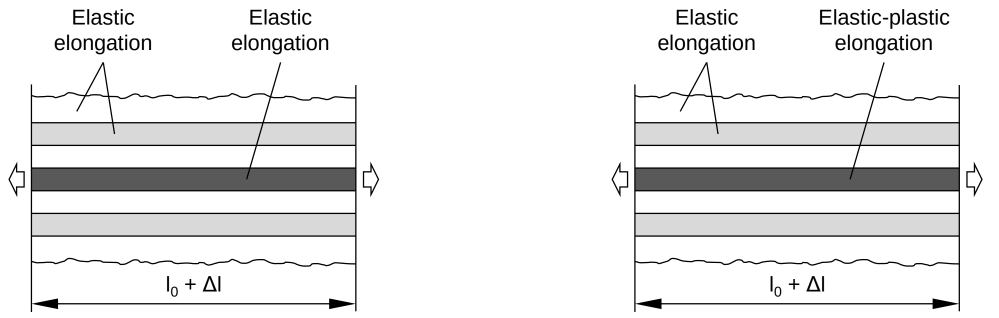

$\Delta l = l_0 \cdot \varepsilon,\ 0 < \varepsilon < \varepsilon_{yield,SF},\ \varepsilon_{SF} = \varepsilon$

State 1: Uniform elastic elongation

$\Delta l = l_0 \cdot \varepsilon,\ \varepsilon_{yield,SF} < \varepsilon < \varepsilon_{max,CF},\ \varepsilon_{SF} = \varepsilon$

State 2: Uniform elastic-plastic elongation

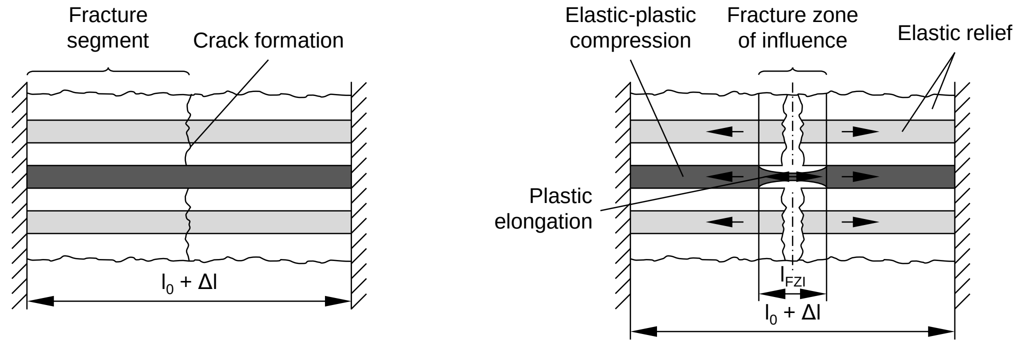

$\Delta l = l_0 \cdot \varepsilon,\ \varepsilon \rightarrow \varepsilon_{max,CF},\ \varepsilon_{SF} = \varepsilon$

State 3: Failure initiation

$\Delta l = l_0 \cdot \varepsilon,\ l_{FZI} = f_{FZI} \cdot (l_0 + \Delta l),\ \varepsilon = \varepsilon_{max,CF},\ \varepsilon_{max,CF} < \varepsilon_{FZI,SF} < \varepsilon_{max,SF}$

State 4: Fracture gap generation

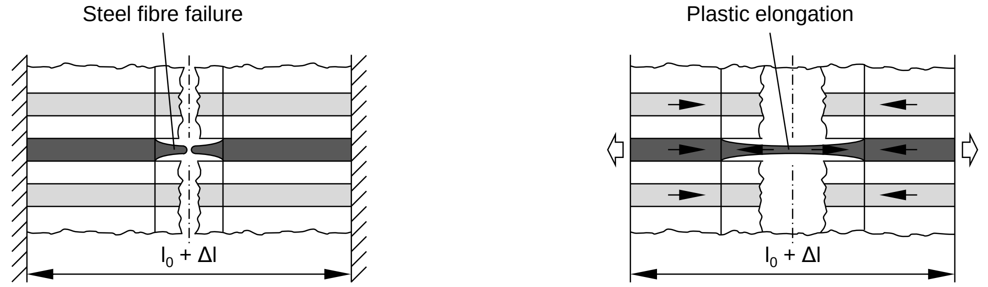

$\Delta l = l_0 \cdot \varepsilon,\ \varepsilon = \varepsilon_{max,CF},\ \varepsilon_{FZI,SF} > \varepsilon_{max,SF}$

State 5: Brittle composite failure ($f_{FZI} < f_{FZI,crit}$)

$\Delta l = l_0 \cdot \varepsilon,\ \varepsilon_{max,CF} < \varepsilon < \varepsilon_{max,SF},\ \varepsilon_{max,CF} < \varepsilon_{FZI,SF} < \varepsilon_{max,SF}$

State 6: Post-failure yielding ($f_{FZI} > f_{FZI,crit}$)

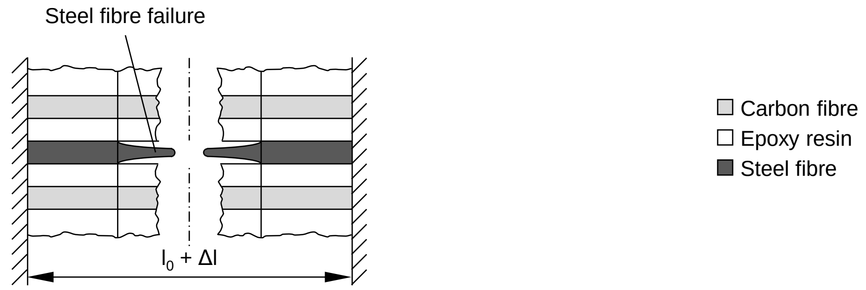

$\Delta l = l_0 \cdot \varepsilon,\ \varepsilon_{max,CF} < \varepsilon < \varepsilon_{max,SF},\ \varepsilon_{FZI,SF} > \varepsilon_{max,SF}$

State 7: Quasi-ductile composite failure ($f_{FZI} > f_{FZI,crit}$)

Figure 2. Schematic illustration of the failure process of a UD hybrid composite under tensile load in parallel to its fibre orientation [1]

State 2: After exceeding their yield strain, the stainless steel fibres are plastically elongated. Their deformation, however, still occurs uniformly on the entire length of the loaded composite. Onset of plastic deformation leads to a degradation of the stiffness of the steel fibres and thus of the hybrid composite. The progressive elongation of the composite causes further storage of elastic energy by CFRP and permanent energy absorption by plastic deformation of the steel fibres.

State 3: The global elongation of the composite and thus of each constituent equates to the elongation at break of the carbon fibres. This causes tensile failure initiation of the carbon fibres and the epoxy resin. For small steel fibre percentages, the stress at this elongation conforms to the tensile strength of the hybrid composite. Due to their higher elongation at break, the (so far) uniformly elongated steel fibres remain as load-bearing part of the composite.

State 4: The failure of the carbon fibres and the epoxy resin leads to an elastic unloading of the fracture halves. This highly transient process occurs without global change in length of the composite but exclusively by relative displacement between its constituents. In this context, two different areas in the composite have to be distinguished: Over a certain length in the proximity of the growing fracture gap, the steel fibres can deform freely (no fibre-resin-adhesion). This area is denominated as **fracture zone of influence (FZI)**. Outside this area, the steel fibres are bonded to the surrounding material. Within the FZI, the carbon fibres and the epoxy resin are completely elastically relieved. Conversely, the steel fibres in this area are further elongated to bypass the growing fracture gap. Outside the FZI, the steel fibres are elastically relieved or even elastic-plastically compressed due to the elastic spring-back of the adhesive surrounding CFRP. The relaxation of the CFRP in this area is, however, incomplete due to the permanent deformation of the steel fibres outside and the tensile load exerted by the steel fibres inside the FZI. The degree of the remaining deformation depends on the extent of the FZI as well as the share and the properties (strain hardening) of the embedded steel fibres. The totality of released elastic energy is dissipated by inter-fibre-failure, fibre fracture, fragmentation and friction between arising laminate bundles or yielding of the embedded steel fibres.

State 5: During the energy transfer, the steel fibres within the FZI fail if they are strained beyond their elongation at break. In this case, ultimate failure of the hybrid material occurs without any further global elongation since failure initiation. Macroscopically, the hybrid composite then exhibits a brittle failure behaviour (similar to CFRP). The elongation at break corresponds to that of the carbon fibres.

State 6: If the energy redistribution during the fracture gap generation causes an elongation of the steel fibres within the FZI without exceedance of their strain at failure, the hybrid composite sustains its structural integrity and can bear further global deformation after failure of the carbon fibres, albeit on a lower level of load. The hybrid composite then exhibits pronounced post-failure behaviour. Progressive elongation of the composite is accompanied by hardening of the steel fibres, hence re-gain of the mean composite stress. Simultaneously, increasing tensile stress of the steel fibres within the FZI causes a slight rise of the elongation of the fracture halves.

State 7: Ultimate failure of the hybrid composite finally occurs after local (within the FZI) exceedance of the strain at failure of the reinforcing steel fibres. However, since the steel fibres primarily yield within the FZI (heterogeneous strain distribution of the composite) the global elongation at break of the composite falls below the one of the dry steel fibres. In the remaining parts of the composite, the available ductility of the steel fibres is far from being exhausted.

According to this theoretical model, the macroscopic failure pattern (brittle failure or pronounced after-damage stage) of the hybrid composite is determined by the size of the fracture gap generated and whether the integrated steel fibres are capable of bypassing this gap. This depends on various parameters, in particular the extent of the fracture zone of influence (i.e. the steel fibre-resin-adhesion), the strain at failure of the applied steel fibres, the ratio of steel to carbon fibres, the effective stiffness of the surrounding CFRP and the strain hardening (or strength) of the steel fibres. A structural-dynamic analysis of the fracture gap formation allows to predict the post-damage stress-strain relation in dependence on those parameters [9]. A simplification by means of a disregard of the dynamic components (energy dissipative shares) allows to efficiently estimate the post-damage stress-strain relation.

3. Application to a UD hybrid composite

In this way, the stress-strain relation of a tensile-loaded UD hybrid composite is exemplarily estimated. The steel fibres are distributed homogenously in the entire volume of the composite. The volume shares of the constituents are given in table 1.

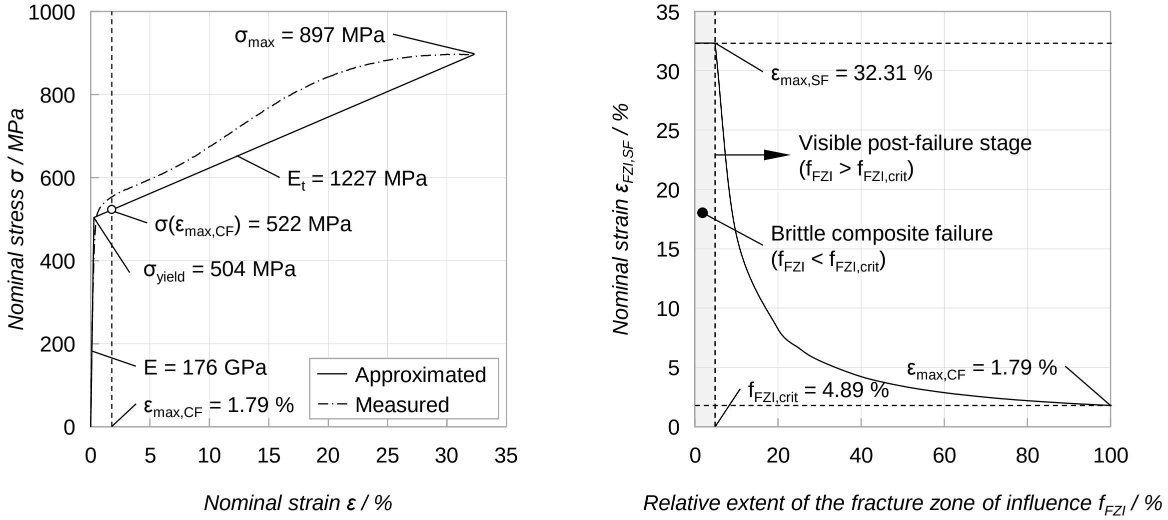

Figure 3. (left) Bi-linear approximation of the stress-strain relation of the stainless steel fibres and (right) resulting elongation of the stainless steel fibres within the fracture gap as a function of the fracture zone of influence [1]

For this estimation, the non-linear stress-strain relation of the steel fibres is approximated by a bilinear elastic-plastic material behaviour, figure 3 (left). The carbon fibres and the epoxy resin are assumed to exhibit a linear elastic stress-strain relation. Moreover, the epoxy resin is set to fail simultaneously with the carbon fibres. For convenience, both constituents are combined to one phase denominated as (surrounding) CFRP. The corresponding properties are calculated by the linear rule of mixtures. Any strain rate sensitivity is neglected. Furthermore, the analytical model postulates similar stress-strain relation under tensile as well as compression load for each constituent. The assigned characteristics are summarised in table 1.

Table 1. Properties of the composite's constituents applied for the analytical approach [1]

Material	E / GPa	σ_{yield} / MPa	ε_{yield} / %	σ_{max} / MPa	ε_{max} / %	φ / vol.%
Carbon fibre	240	-	-	4300	1.79 [a)]	49.1
Epoxy resin	3.52	-	-	63 [a)]	1.79 [b)]	32.1
CFRP	147	-	-	2625	1.79	81.2
Steel fibre	176	504	0.29	897	32.31	18.8

[a)] adapted for an ideal linear elastic material behaviour abiding Hooke's law ($\varepsilon_{max,CF} = \sigma_{max,CF} / E_{CF}$ and $\sigma_{max,R} = E_R \cdot \varepsilon_{max,R}$)

[b)] adapted to the strain at failure of the carbon fibres ($\varepsilon_{max,R} \overset{!}{=} \varepsilon_{max,CF}$)

In principle, two steady states of the hybrid composite are considered in order to approximate the post-damage stress-strain relation of the composite: the state immediately before failure initiation (state 1) and the state after load redistribution (state 2), figure 4.

State 1: Right before failure initiation, the elongation of each constituent equates to the global elongation of the composite and corresponds to the elongation at break of the carbon fibres. At this state, both the carbon fibres and the epoxy resin are elastically elongated. The steel fibres, by contrast, are already plastically deformed (uniformly on their entire length) since their yield strain is smaller than the current global elongation of the composite.

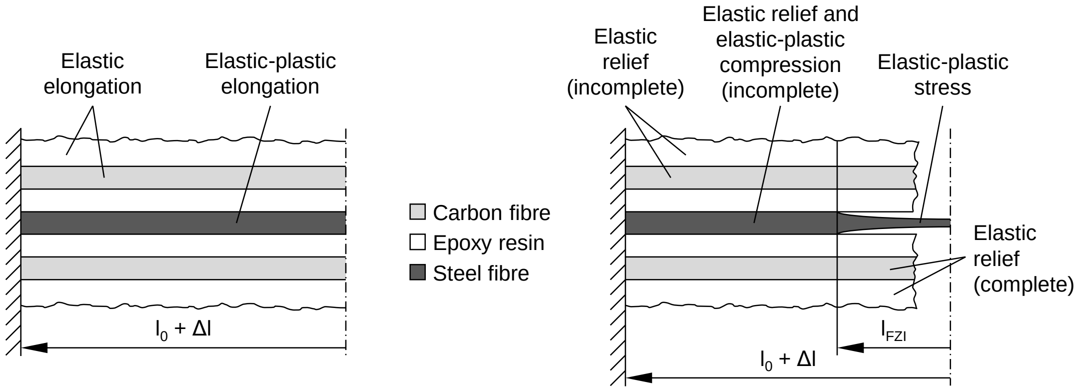

$\Delta l = \varepsilon \cdot l_0,\ \varepsilon \rightarrow \varepsilon_{max,CF},\ \varepsilon > \varepsilon_{yield,SF}$

State 1: Before failure initiation

$\Delta l = \varepsilon \cdot l_0,\ l_{FZI} = f_{FZI} \cdot (l_0 + \Delta l),\ \varepsilon = \varepsilon_{max,CF},\ \varepsilon_{FZI,SF} > \varepsilon$

State 2: After fracture gap generation

Figure 4. Illustration of the material states for the derivation of the stress-strain relation of the UD hybrid composite in parallel to its fibre orientation [1]

State 2: Immediately after the load redistribution (no global change in length of the composite since state 1), the carbon fibres and the epoxy resin within the fracture zone of influence are relieved (unrestrained elastic relaxation). By contrast, the steel fibres in this area are further elongated to bypass the fracture gap generated. Outside the fracture zone of influence, the steel fibres (which are bonded to the surrounding CFRP) are first elastically relieved and then, if necessary, elastic-plastically compressed due to the elastic spring-back of the surrounding CFRP. The relaxation of the CFRP in this area is, however, incomplete due to the permanent deformation of the steel fibres outside and the tensile load exerted by the steel fibres inside the fracture zone of influence.

The critical length of the fracture zone of influence (given relatively to the length of the loaded composite) is determined iteratively, assuming that the steel fibres within the fracture zone of influence are strained to their maximum elongation and having regard to three principal assumptions:

(1) The transition of the limit states occurs exclusively by means of relative displacement between the steel fibres and the surrounding CFRP, i.e. without change in length of the composite (**kinematic boundary condition**).

(2) The normal force executed on the laminate fragments outside the fracture zone of influence equals the normal force of the steel fibres in the fracture zone of influence (**balance of forces**).

(3) The fracture halves return to their steady state without oscillation (critically damped or overdamped harmonic oscillator). Since the relief motion starts without initial velocity, overshoots of the fragments over their final (steady) position do not occur. Damping (energy dispersion) is given by yielding of the steel fibres as well as inter-fibre-failure, fibre fracture and friction between laminate bundles.

According to this theoretical model, failure is initiated independently of the steel fibre fraction and the size of the fracture zone of influence at a global elongation of 1.79 %. At this elongation, the hybrid composite exhibits a heterogeneous stress distribution with a local stress of 522 MPa at the steel fibres and 2625 MPa at the surrounding CFRP. With the given proportion, this corresponds to an average stress of 2230 MPa. As shown at the end of this section, this stress conforms to the ultimate tensile strength of the hybrid composite. The degree of local elongation of the steel fibres within the fracture zone of influence for bridging the propagating fracture gap directly depends on the extent of the fracture zone of influence f_{FZI}. The smaller the fracture zone of influence, the higher is the local elongation of the steel fibres and thus the lower is the residual elongation capacity of the hybrid composite, i.e. its ultimate strain at failure. In case of $f_{FZI} = 100$ %, the steel fibres and the surrounding CFRP can be considered as independent of each other. Failure initiation is accompanied by complete elastic unloading of the CFRP portion without affecting the steel fibres. During the fracture gap generation, the uniform elongation of the steel fibres therefore remains unchanged at 1.79 %. Subsequently, the composite can sustain further elongation up to an ultimate failure strain which equates

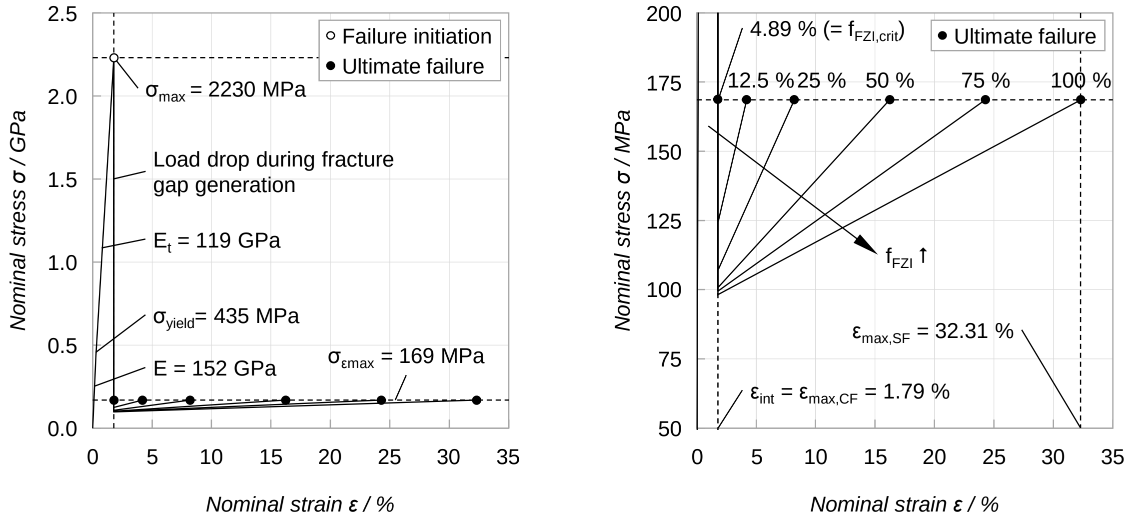

Figure 5. Stress-strain relation of the UD hybrid composite of type SCFRP 20h UD in parallel to its fibre orientation as a function of the fracture zone of influence: (left) overall view and (right) close-up view of the post-damage stage [1]

to the strain at failure of the incorporated steel fibres. In case of $f_{FZI} = f_{FZI,crit}$, the steel fibres within the fracture zone of influence are strained by the elastic spring-back of the fracture halves to their maximum elongation of 32.31 %. According to this definition, a critical length of the fracture zone of influence of 4.89 % is determined for the considered hybrid composite. For this limit state, the residual deformability of the hybrid composites becomes minimal; its ultimate strain at failure equals the elongation at break of the carbon fibres. In case of $f_{FZI} < f_{FZI,crit}$, the local elongation of the steel fibres within the fracture zone of influence exceeds their strain at failure during fracture gap generation; the composite consequently exhibits brittle failure. In principle, the elongation of the steel fibres within the fracture zone of influence is accompanied by strain hardening, i.e. a local stress increase. The smaller the fracture zone of influence, the greater is the strain hardening of the steel fibres and thus the less pronounced is the load drop during failure of the carbon fibres. In case of $f_{FZI} = 100$ %, the steel fibres show a local stress of 522 MPa immediately after the fracture gap generation. This corresponds to a global stress of 98 MPa (considering the steel fibre share). If the fracture zone of influence is reduced to $f_{FZI} \leq f_{FZI,crit}$, the steel fibres are stressed to 897 MPa, which equates to a global stress of 169 MPa. Independently of f_{FZI}, ultimate failure of the composite occurs at a local stress of the steel fibres of 897 MPa, which again corresponds to a global stress of 169 MPa. The ultimate tensile strength of the considered hybrid material is therefore defined by the stress at the moment of failure initiation.

Table 2. Characteristic values of the UD hybrid composite of type SCFRP 20h UD as a function of the fracture zone of influence [1]

f_{FZI} / %	ε_{int} / %	σ_{max} / MPa	σ_{SF} / MPa a)	ε_r / % b)	$\sigma_{FZI,SF}$ / MPa c)	σ / MPa c)	ε_{max} / %	$\sigma_{\varepsilon max}$ / MPa
< $f_{FZI,crit}$	1.79	2230	522	-	-	-	1.79 (= $\varepsilon_{max,CF}$)	169
4.89 (= $f_{FZI,crit}$)	1.79	2230	522	0.22	897 (= $\sigma_{max,SF}$)	169	1.79 (= $\varepsilon_{max,CF}$)	169
12.5	1.79	2230	522	0.19	660	124	4.34	169
25	1.79	2230	522	0.18	582	109	8.35	169
50	1.79	2230	522	0.17	542	102	16.38	169
75	1.79	2230	522	0.17	529	99	24.42	169
100	1.79	2230	522	0.00	522	98	32.31 (= $\varepsilon_{max,SF}$)	169

a) right before failure of the carbon fibres (state 1)

b) elongation of the fracture halves in steady state 2

c) immediately after fracture gap generation (state 2)

In addition to the critical length of the fracture zone of influence, this analytical procedure yields all characteristic values which are required to approximate the stress-strain relation of the UD hybrid composite in parallel to its fibre direction as a function of the fracture zone of influence (i.e. the steel fibre-resin-adhesion) and the properties of the composite's constituents, figure 5 and table 2. For the genuine case of an underdamped system, the steel fibres within the fracture zone of influence are more elongated during the fracture gap generation. By trend, this shifts the post-damage stress-strain relation towards smaller values of the fracture zone of influence.

5. Conclusion

Hybrid composites comprising both brittle and ductile continuous reinforcing fibres exhibit complex failure behaviour. To theoretically predict the entire failure process, a novel analytical approach is introduced, which is based on a structural-dynamic analysis of the fracture gap formation. Basically, the analytical approach yields all characteristic values to approximate the stress-strain relation of the UD hybrid composite in parallel to its fibre orientation as a function of the fracture zone of influence (i.e. the steel fibre-resin-adhesion), the steel fibre share and the properties of the hybrid composite's constituents. Other parameters, such as the attenuation of the fracture segment's movement must be (experimentally) estimated. Further simplifications, however, allow a sufficiently accurate estimation of the material behaviour without specifying these difficult-to-determine characteristic values. In any case, the estimation requires an iterative calculation.

Acknowledgements

The financial support for this study was provided by the German Research Foundation (DFG BR 4262/2-1 and BA 4073/6-1) and the Federal Ministry of Education and Research Germany (BMBF 03X3042D). Prepreg and resin film was kindly supplied by Cytec Engineered Materials GmbH.

References

[1] B. Hannemann. Multifunctional metal-carbon-fibre composites for damage tolerant and electrically conductive lightweight structures. IVW-Schriftenreihe, 128, Kaiserslautern, 2018.

[2] Y. Mosleh, D. Clemens, L. Gorbatikh, I. Verpoest, A. W. van Vuure. Penetration impact resistance of novel tough steel fibre-reinforced polymer composites. Journal of Reinforced Plastics and Composites, 2015, 34 (8), 624-635.

[3] B. Lehmann, S. K. Selvarayan, R. Ghomeshi, G. T. Gresser. Carbon fiber reinforced composite - Toughness and structural integrity enhancement by integrating surface modified steel fibers. Materials Science Forum, 2015, 825, 425-432.

[4] M. G. Callens. Development of ductile stainless steel fibre composites. Leuven, 2014.

[5] U. P. Breuer, S. Schmeer. Carbon and metal-fiber-reinforced airframe structures. In: K. Friedrich, U. P. Breuer (Eds.). Multifunctionality of polymer composites. Elsevier, 2015.

[6] B. Hannemann, S. Backe, S. Schmeer, F. Balle, U. P. Breuer, J. Schuster. Hybridisation of CFRP by use of continuous metal fibres (MCFRP) for damage tolerant and electrically conductive lightweight structures. Composite Structures, 2017, 172, 374-382.

[7] L. Utzig, C. Karch, J. Rehra, B. Hannemann, S. Schmeer. Modelling and simulation of effective strength of hybrid polymer composites reinforced by carbon and steel fibres. Journal of Materials Science, 2017, 53 (1), 667-677.

[8] C. Bauer, B. Hannemann, E. Glatt, S. Schmeer. Micromechanical simulation of a multifunctional hybrid composite with continuous steel and carbon fibre reinforcement. 17th Automotive Composites Conference and Exhibition, Detroit, 06.-08.09.2017.

[9] J. Rehra, B. Hannemann, S. Schmeer, J. Hausmann, U. P. Breuer. Approach for the analytical description of the post-damage behaviour of steel and carbon fibre reinforced hybrid composites.

Advanced Engineering Materials, 2018.